Final Report for

DoE Grant DE-FG02-99ER41107

Studies of High Energy Particle Astrophysics

Department of Physics
Michigan Technological University
Houghton, Michigan 49931

PI: David F. Nitz

Address: Physics Department
Michigan Technological University
1400 Townsend Dr.
Houghton, MI 49931

Telephone: 906 487 2274

Email: dfnitz@mtu.edu

1 Introduction

This report covers the progress during the period April 15th, 2011 through April 30th, 2014.

The principal investigator is Professor David Nitz. Professor Brian Fick is the Co-PI. Other members include researcher Johana Chirinos Diaz, and PhD students Tolga Yapici and Niraj Dhital. The focus of the group is the study of the highest energy cosmic rays using the Pierre Auger Observatory.

The major goals of the Pierre Auger Observatory are to discover and understand the source or sources of cosmic rays with energies exceeding $10^{19} eV$, to identify the particle type(s), and to investigate the interactions of those cosmic particles both in space and in the Earth's atmosphere. The Pierre Auger Observatory in Argentina was completed in June 2008 with 1660 surface detector stations (SD)[1] and 24 fluorescence telescopes arranged in 4 stations (FD) [3]. It has a collecting area of 3,000 km^2, yielding an aperture of 7,000 $km^2 \cdot sr$. Plans are underway for a possible upgrade of the Observatory.

A major science result from the Auger Observatory has been the discovery that the arrival directions of the highest energy cosmic rays (above 55 EeV) are not isotropic. The in-homogeneous distribution of matter in the local universe appears to be imprinted in the anisotropy of their arrival directions [4].

These particles are above the energy threshold where interactions with photons of the cosmic microwave background (CMB) are expected to limit the range of cosmic rays. Energy loss by pion photo-production was predicted by Greisen [5] and by Zatsepin and Kuzmin [6] shortly after the discovery of the CMB in 1965 [7]. Photo-disintegration of nuclei can produce a similar effect on the cosmic ray energy spectrum [8]. The steepening of the energy spectrum near 40 EeV, measured with the High Resolution Fly's Eye (HiRes) [9, 10] as well as the Auger Observatory [11, 12], is consistent with the expected energy loss due to the CMB. However, it could be attributed to a feature of the average particle injection spectrum instead of energy losses during propagation. The correlation of arrival directions with the large-scale matter distribution inside the GZK sphere of 75 Mpc confirms that cosmic rays from the nearly isotropic visible universe beyond the GZK sphere are indeed strongly suppressed.

Fluorescence measurements of the depth of shower maximum (X_{max}) for energies up to 35 EeV, the maximum that can be reached with the aperture of the Auger Observatory, show striking trends [13]. These results, when analyzed using current hadronic interaction models, suggest an increasingly heavy (iron-rich) composition, but this interpretation is astrophysically difficult to explain, especially in view of the anisotropy that becomes apparent at somewhat higher energy. Furthermore, when the details of the X_{max} distribution are included in the analysis (rather than just the average), a 2 component transition from light to heavy composition is disfavored. Addition of the measured muon component of the showers, which shows a constant relative excess compared to model calculations, independent of energy, further enriches this puzzle.

[1] There is an infill [1] enhancement which locates 46 of the 1660 stations on a smaller grid. Coupled with an associated extension of the fluorescence telescopes [2], this provides hybrid measurements down to $10^{17} eV$.

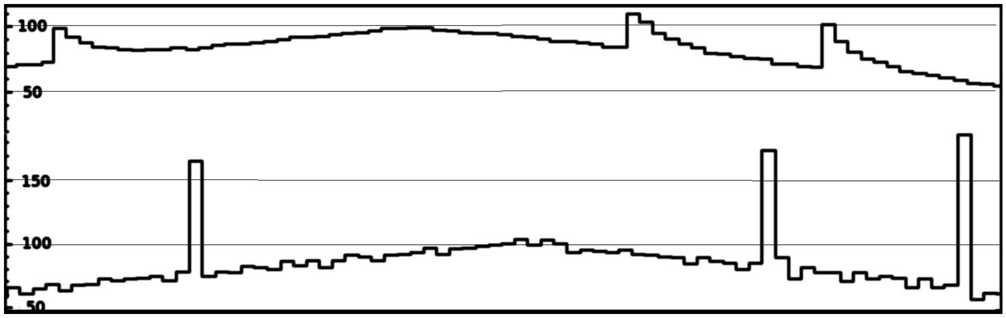

Figure 1: Verilog simulation of the actual PLD configuration of the deconvolution of the signal for the ToTd trigger. The top trace shows the input signal to the trigger, illustrating three muons above a smoother electromagnetic background. The bottom trace shows the deconvolved trace upon which the pulse height window is applied. The muon signal has been concentrated in one or two bins, while the shape and amplitude electromagnetic portion of the signal remains unaltered. The vertical scale is in units of FADC counts, while each horizontal bin is 25 ns.

2 Research Activities during 2013/14

Activities during the past year included operation of the Auger Observatory, advances in atmospheric monitoring techniques, improvements to the surface array trigger, and analysis efforts aimed at both interpretation of the data and improved monitoring.

2.1 SD Trigger

During the past year, we (Nitz) have completed work on additional Auger Observatory Surface Detector level 1 triggers in conjunction with primarily our French colleagues at the University of Paris VI. The MTU group coordinated the effort, and performed the implementation of the triggers in the SD front-end electronics firmware. The new triggers have been installed on the full array and the data stream now includes the new triggers. The new triggers have been added to the monitoring database, and additional monitoring displays have been implemented.

The signals from each of the 3 9" PMTs in each SD water Cerenkov detector are recorded at a 40 MHz rate by flash ADCs (FADCs). Programmable logic devices (PLDs) on the front-end board in the surface detector electronics generate the lowest level surface detector triggers using these FADC traces. Until recently, two main triggers have been employed: 1) a simple threshold trigger on the amplitude of the signal in at least 2 of the 3 PMTs, and 2) a time-over-threshold (ToT) which requires that 13 or more of the 25 ns time bins within a $3\,\mu$s sliding window be above a signal of 0.2 vertical equivalent muons (VEM) in 2 of the 3 PMTs [14, 15]. This latter trigger has proved to be extremely powerful and pure. In June 2013, the Auger Observatory installed across the entire array two additional SD triggers implemented by Nitz. These triggers build upon the ToT trigger in two directions, applying

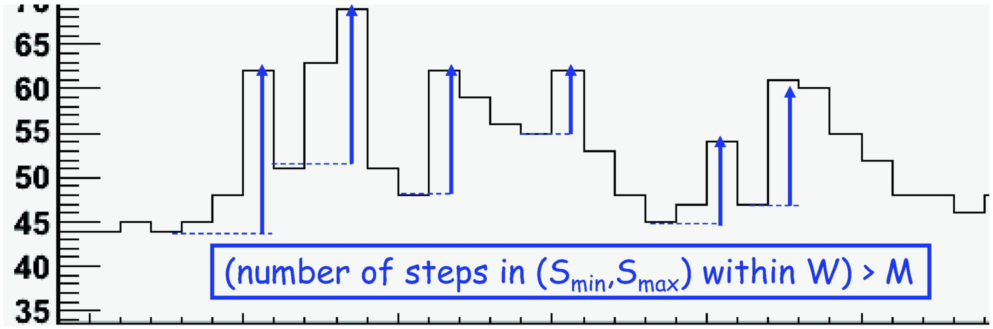

Figure 2: Concept of the MoPS trigger.

more sophisticated analysis to the FADC traces.

The time-over-threshold-deconvolved (ToTd) trigger deconvolves the the exponential tail of the diffusely reflected Cerenkov light pulses before applying the ToT condition. This has the effect of reducing the influence of muons in the trigger, since the typical signal from a muon, with fast rise time and $\approx 60\,$ns decay constant, is compressed into one or 2 time bins. This is illustrated in Fig. 1

The multiplicity-of-positive-steps trigger (MoPS), on the other hand, counts the number of positive going signal steps in 2 of 3 PMTs within the $3\,\mu$s sliding window (see Fig. 2). The steps are required to be above a small FADC value (≈ 5 times RMS noise) and below a moderate value ($\approx \frac{1}{2}$ vertical muon step). This reduces the influence of muons in the trigger. Both the ToTd and MoPS triggers also require the integrated signal to be above ≈ 0.5 VEM.

Because these triggers minimize the influence of single muons, they reduce the energy threshold of the array, while keeping random triggers at an acceptable level. Thus they improve the energy reach of the SD, as well as improve the trigger efficiency for photon and neutrino showers. The increased efficiency for a single station trigger from the new triggers for small signals is shown in Fig. 3.

2.2 Atmospheric Monitoring

The Auger Observatory employs a number of instruments, the Central Laser Facility (CLF) [17], the eXtended Laser Facility (XLF), LIDARs [18], and IR cameras [19], to identify clouds over the array. The MTU group (Chirinos) developed a complementary cloud identification system based on infrared measurements performed by geosynchronous satellites. The system provides cloud probabilities for a 360-element grid of 2.5 km$\times$5.2 km regions encompassing the area of the observatory, twice per hour (see Fig. 4). The MTU group is in charge of collecting this information from the NOAA website, processing it, and placing it into a database for use by the rest of the collaboration.

Two important features of this work are 1) the raw data is freely available for the entire running period of the Auger Observatory, and 2) the Auger Central Laser Facility (CLF)

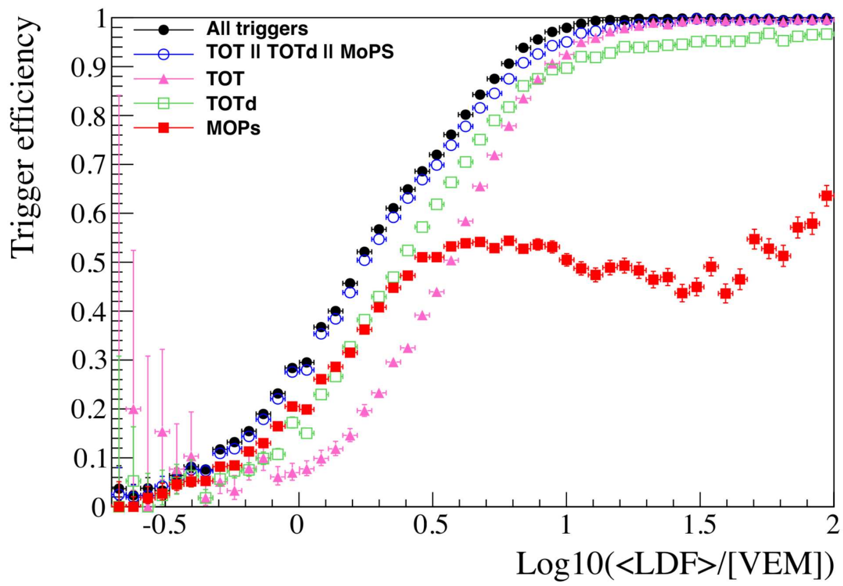

Figure 3: Single station trigger probability for various triggers versus the integrated signal size in units of "vertical equivalent muons" [16].

provides a unique ability to ground-truth the cloud detection algorithm developed at MTU, quantifying the accuracy of the method and demonstrating an improvement over previously available algorithms.

All the data obtained since early 2004 (for FD running periods) have been processed and loaded into the GOESDB portion (developed at MTU) of the Auger atmospheric monitoring database. In collaboration with Northeastern University, we implemented the database handler for the GOESDB, to fully incorporate it into the Auger OffLine analysis structure. As an example of the use of this information we created a map of clear fraction observations for each ground pixel covering the observatory for FD running periods between 2007 and late 2011 (See Fig. 4).

The MTU group was in charge of publishing this work as a full author list Auger Collaboration paper [20].

We have started to expand this work to include a comparison of the method with cloud identifications made by the four LiDAR devices at the FD sites.

2.3 Exotic Search

Ultra High Energy Cosmic Rays (UHECR) provide us an opportunity to explore the unprecedented aspect of particle physics. With various proposed models of particle interactions and possible extension of Standard Model (SM) to Supersymmetric Models (SSM), the UHECR air showers open up new windows to study physics of particle interactions at energies much higher than that in the Large Hadron Collider (LHC) experiment. Many of these proposed

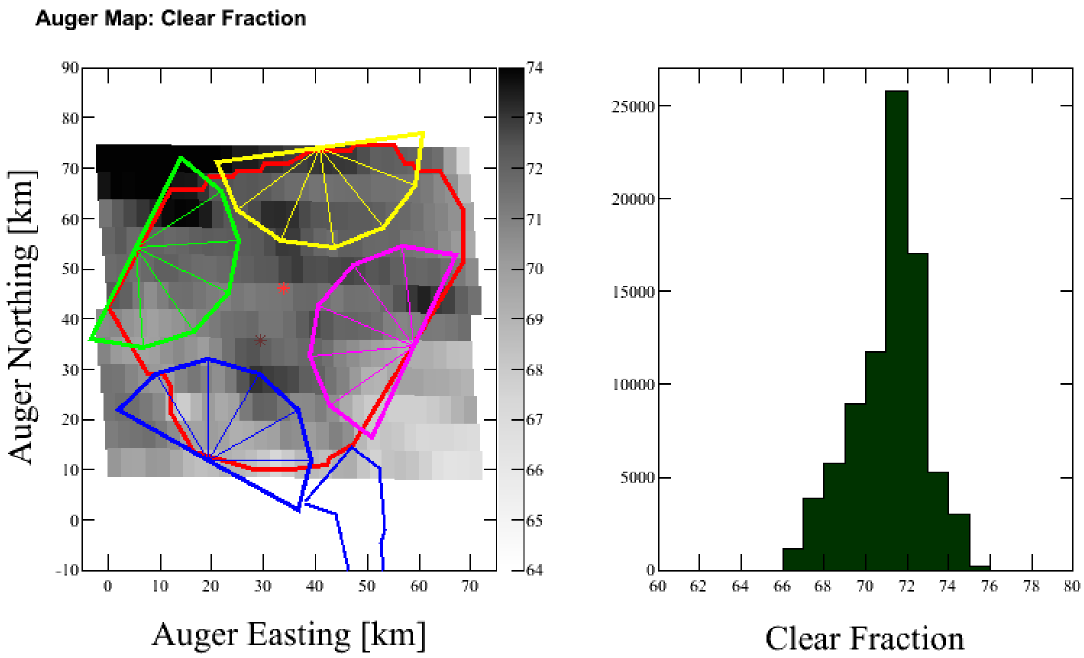

Figure 4: Left - Clear fraction map between 2007 and 2011. Right - Clear fraction frequency for all pixels between 2007 and 2011.

models predict the production of heavy particles with lifetimes which may be of the order of picoseconds to about a nanosecond[21]. As an example, gravity-mediated supersymmetry with R-parity violation allows the decay of lightest supersymmetric particle within the lifetime of this range [22]. In gauge-mediated supersymmetry models, next-to-lightest supersymmetric particle may exhibit this property [23]. There are several other models which predict such particles [24, 25, 26, 27]. Fig. 5(left) illustrates a scenario where an unknown weakly interacting massive particle is produced in the first interaction of primary particle with air nucleus at an atmospheric depth X_1, which travels invisibly for a distance L and decays at an atmospheric depth X_1' producing a second shower superimposed to the first(double-bump profile). For such situations, the longitudinal shower profile has two maxima, separation and amplitude of which are determined mainly by lifetime and energy of the particle created. It is trivial to estimate the ratio of two fundamental properties, mass(m) and lifetime(τ) of the particle, if one can measure energy and the separation between the production position and decay position of the exotic particle. Fig. 5(right) shows the contours of $\frac{m}{\tau}$ for exotic particle as a function of its energy and decay position, for a zenith angle of 70°.

Motivated by relatively larger volume of SD data and its reconstruction being independent on atmospheric and weather conditions we are performing a search for such exotic particles using the SD data. We simulate double-bump air showers for such scenarios using CORSIKA [28]. Two sets of showers are simulated, first set comprising of normal proton showers,

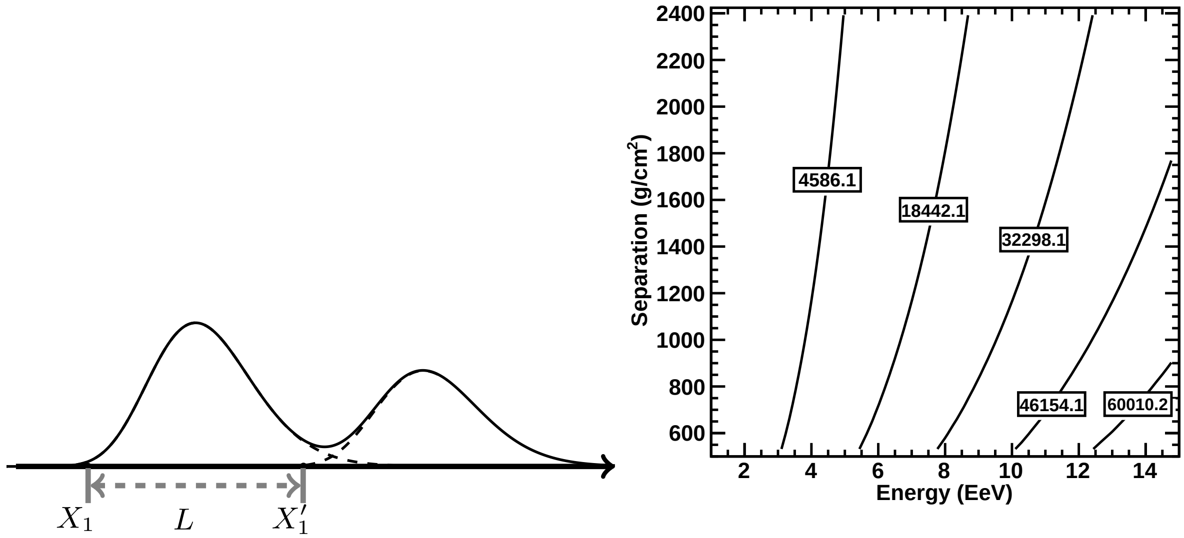

Figure 5: Left: Schematic of production depth profile of secondary particles for air shower in which weakly interacting massive particle decays later Right: Contours of $\frac{m}{\tau}$ (in $\frac{GeV/c^2}{ns}$) for exotic particle as a function of its energy and decay position, assuming that the zenith angle of primary particle is 70°.

and the second set comprising of the proton showers with deeper injection depths. A final distribution of particles at ground is obtained by combining the two CORSIKA generated showers adjusting the time of injection of the second set to match that of first. We used zenith angles of 60°, 65°, 70° and 75° for the simulations.

Starting from the arrival times and positions of particles at the ground we reconstruct the production depths of the particles that arrive to the ground, assuming that the particles travel with the speed of light. In reality, muons in the cosmic ray air showers tend to arrive earlier than the electromagnetic component which suffers from multiple scattering. Moreover, significant fraction of particles from the earlier part of the shower is lost on its way to ground compared to the later part of the shower. This further enhances the later part of the shower, making the contribution of the exotic particle more apparent. In Fig. 6(left), production depth of particles from the normal shower (25 EeV, 70°) is shown in green, production depth of particles from the deeper shower (8 EeV, injection depth 1500 g/cm^2) is shown in blue, and that from the combined shower is shown in red. These are obtained using the output from CORSIKA without performing a detector simulation. Fig. 6(right) shows the distribution after a full detector simulation of the combined shower.

This work is the basis of Niraj Dhital's thesis.

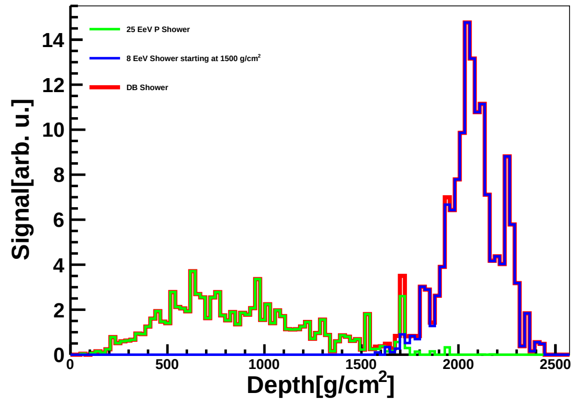

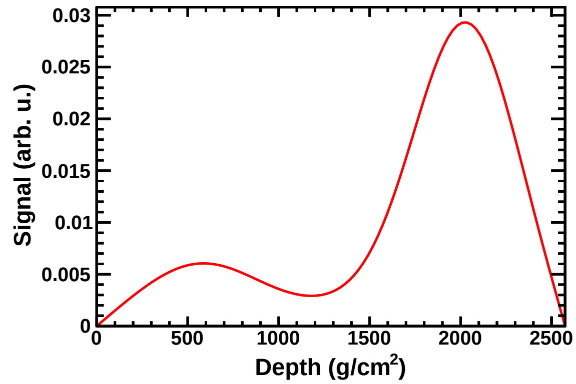

Figure 6: Left: Production depth of particles that arrive to the ground obtained from the ground particles information of CORSIKA output (without detector simulation). Right: Production depth for the same shower after performing SD simulation.

2.4 Hadronic Interactions

The extensive air shower development depends on the primary particle initiating the shower. The distribution of the first interaction length of the primary particle is one of the main reasons for the large fluctuation in shower observables [29]. Embedded information in the shower development can be extracted using different methods. Our group employed an Artificial Neural Network (ANN) prediction model which incorporates the shape of the shower development, particularly muon production depth profile. In addition to event-by-event based predictions, cumulatively the results yield the distributions of first interaction lengths (see Fig. 7). These distributions provide information about the mean-free paths, and in return the cross-sections, of the primary particles in the mixture.

According to the hypothesis of a transition from light primary particles to heavier ones at high energies ($E>10^{18.5}$ eV), cosmic rays may be composed of multiple primaries at different energy intervals. Thus, solely, the results of the prediction model cannot be interpreted for finding the cross-section of the cosmic rays. Due to the fact that heavier cosmic rays have a shorter tail in their first interaction length distributions, segmenting the distribution makes it possible to identify the mean-free paths of the cosmic rays in the mixture. Through Monte-Carlo simulations of p→CNO→Fe at different mixing rates, our group computed two breaking points to divide the distributions.

The statistical and systematic errors of using breaking points on calculation of mean-free paths at different compositions are being carried out. In addition, detector simulations are being carried out for the application of the prediction model and its interpretation.

This work is the basis of Tolga Yapici's thesis.

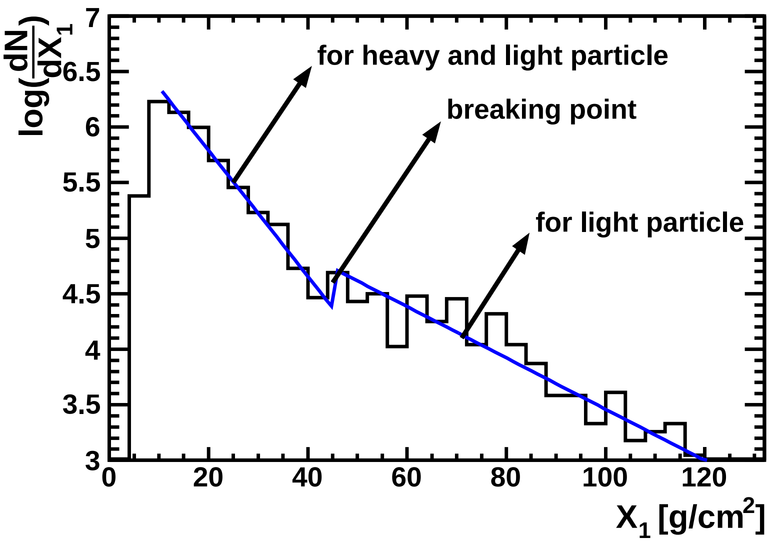

Figure 7: A sample distribution of first interaction length values for an arbitrary mixed composition in semi-log scale.

3 Research Activities during 2012/13 and 2011/2012

Activities during these years included operation of the Auger Observatory, advances in atmospheric monitoring techniques, improvements to the surface array trigger, and analysis efforts aimed at both interpretation of the data and improved monitoring.

3.1 SD Trigger

During these years, we (Nitz) worked on developing additional Auger Observatory Surface Detector level 1 triggers in conjunction with primarily our French colleagues at the University of Paris VI.

Based upon results of testing in 2011, we requested and were granted permission in November, 2011 to install the ToTd trigger, along with associated modifications to the monitoring and production analysis packages, in one communications sector of the standard array.

Subsequently, the triggers were tested as previously planned in several different sectors of the array with progressively larger numbers of stations involved in each test. This testing over progressively larger and more diverse areas of the array uncovered some deficiencies with regard to the new triggers and noisy stations As a result, an additional constraint on the integrated signal was added to the new triggers.

3.2 Auger Observatory Communications System

The MTU group (Nitz, Yapici, Kieckhafer) also worked on developing a common communications platform for the Auger Observatory surface instruments, in collaboration with colleagues at KIT (Germany) and KVI (Netherlands).

3.3 Atmospheric Monitoring

We (Chirinos, Yapici, Dhital, and Fick) have provided cloud-cover probability maps for the region of the array and duration of the experiment (see Section 2.2) Initial reports of this work were published as conference proceedings [30, 19].

3.4 Data checks

The AGN correlation at high cosmic ray energies has fallen since the original publication. Between January, 2004 and August, 2007 the AGN correlation rate is remarkably steady at 70% whereupon it abruptly changes to an equally steady 30% (still not consistent with isotropy). We felt it prudent to investigate whether a change in the performance of the instrument was responsible for this behavior. As the anisotropy measurement depends only on shower energy and absolute arrival direction we looked for evidence of changes in the data, between the early and late epoch, that would affect these quantities in such a way as to produce the observed reduction in anisotropy.

We have not been able to reproduce the effect in simulation with plausible shifts in energy calibration, energy resolution, or angular resolution. Additionally, event-by-event comparisons between SD and FD energies for hybrid events showed no change in either scale, variance, or direction resolution, between the two epochs. However, led by initial work at MTU, further studies have verified that there have been small time dependent energy scale changes between the FD and SD. The cause for these drifts is not yet understood, and sorting out how much of the drift is due to the FD and how much to the SD is a work in progress.

There are also hints that there may be a correlation between the apparent change in behavior and two especially cold periods during the austral winters of 2007 and 2010, when ice was observed in the SD stations. One manifestation in the monitoring data is a sharp (over a few weeks) change in the area to peak ratio (A/P) of through-going muon signals. These changes are not yet understood.

When the CLF issues a laser pulse into the atmosphere for FD monitoring, it also both records the energy of the laser with a probe, and sends some of the light to the neighboring SD station (Celeste) over a fiber optic cable. In the hope that this might provide a stable reference, we performed a study of the long term time dependence of the signal measured in Celeste versus the energy measured by the laser probe.

We studied the behavior of the total signal in the tank, the signal in each PMT, the A/P of each PMT and the recovered saturated total signal in the tank in data since 2006. We observed a decrease in the signal coinciding with the drop of A/P during the 2007 and

2010 freezing events. We also see some evidence of a long term decay of the observed laser initiated signal in Celeste (corrected for measured laser energy in the probe), as well as aging of the laser (a decrease in the energy measured by the probe for the same laser voltage).

We also performed simulation studies to try to understand the long term performance of the surface detector array and possible effects on energy reconstruction. We studied both uniform and non-uniform degradation of the liner, and decreases in the water absorption length. None of the studied types of degradation, except for one, produced a reconstructed shower energy shift when the A/P shift was constrained to be consistent with measurements. However, vertically stratified degradation of the water attenuation length could both produce a reconstructed energy shift and keep A/P shifts consistent with measured performance. In situ verification is difficult, and has not yet been performed. This work has been documented in a technical note [31].

3.5 Exotic Search

It has long been conjectured that certain exotic weakly interacting elementary particles could be produced in ultra-high-energy collisions. These particles, once produced, travel invisibly with the normally developing shower cascade until it decays and produces a second shower superimposed on the first (double-bump profile). Other Auger Collaboration groups are actively searching the FD data using this signature. The cloud probability maps produced by MTU (discussed in section 2.2) are important for this work, helping to ensure that any double-bump profiles that might be observed are not simply due to clouds.

We (Fick, Dhital) began a program to perform a more sensitive search using the more voluminous SD data, looking for manifestation in the temporal and spatial structure of the SD events. This is discussed in section 2.3.

3.6 Hadronic Interactions

Our X_{max} results, taken by themselves can be interpreted as either a radical change in chemical composition with rising energy or an equally radical change in hadronic interaction physics. To sort out these possibilities, we (Fick and Yapici) have set out to try to find a means of directly measuring the first interaction depth (X_1) and thus separate composition effects from those of the total cross-section. This is discussed in section 2.4.

BIBLIOGRAPHY AND REFERENCES CITED

References

[1] Alexander Aab et al. The Pierre Auger Observatory: Contributions to the 33rd International Cosmic Ray Conference - The AMIGA muon detectors of the Pierre Auger Observatory: overview and status (ICRC 2013). 2013, 1307.5059.

[2] M. Kleifges for the Pierre Auger Collaboration. Extension of the Pierre Auger Observatory using high-elevation fluorescence telescopes (ICRC 2009). *Proceedings of the 31st International Cosmic Ray Conference, Lodz, 2009*, 2009, 0906.2354.

[3] J. Abraham et al. The Fluorescence Detector of the Pierre Auger Observatory. *Nucl.Instrum.Meth.*, A620:227–251, 2010, 0907.4282.

[4] J. Abraham et al. Correlation of the highest energy cosmic rays with nearby extragalactic objects. *Science*, 318:938–943, 2007, 0711.2256.

[5] Kenneth Greisen. End to the cosmic ray spectrum? *Phys.Rev.Lett.*, 16:748–750, 1966.

[6] G.T. Zatsepin and V.A. Kuzmin. Upper limit of the spectrum of cosmic rays. *JETP Lett.*, 4:78–80, 1966.

[7] Arno A. Penzias and Robert Woodrow Wilson. A Measurement of excess antenna temperature at 4080-Mc/s. *Astrophys.J.*, 142:419–421, 1965.

[8] J.L. Puget, F.W. Stecker, and J.H. Bredekamp. Photonuclear Interactions of Ultrahigh-Energy Cosmic Rays and their Astrophysical Consequences. *Astrophys.J.*, 205:638–654, 1976.

[9] R.U. Abbasi et al. Measurement of the Flux of Ultra High Energy Cosmic Rays by the Stereo Technique. *Astropart.Phys.*, 32:53–60, 2009, 0904.4500.

[10] R.U. Abbasi et al. First observation of the Greisen-Zatsepin-Kuzmin suppression. *Phys.Rev.Lett.*, 100:101101, 2008, astro-ph/0703099.

[11] J. Abraham et al. Observation of the suppression of the flux of cosmic rays above 4×10^{19}eV. *Phys.Rev.Lett.*, 101:061101, 2008, 0806.4302.

[12] J. Abraham et al. Measurement of the energy spectrum of cosmic rays above 10^{18} eV using the Pierre Auger Observatory. *Phys.Lett.*, B685:239–246, 2010, 1002.1975.

[13] J. Abraham et al. Measurement of the Depth of Maximum of Extensive Air Showers above 10^{18} eV. *Phys.Rev.Lett.*, 104:091101, 2010, 1002.0699.

[14] D. Nitz. Triggering and data acquisition systems for the Auger observatory. *IEEE Trans.Nucl.Sci.*, 45:1824–1829, 1998.

[15] D. Nitz. The front-end electronics for the Pierre Auger Observatory surface array. *IEEE Trans.Nucl.Sci.*, 51:413–419, 2004.

[16] Maris Settimo, Billoir and Molina Bueno. Trigger probability for single stations and air-showers with the TOTd and MoPS algorithms . *Auger internal report GAP 2013-114*, 2013.

[17] Pedro Abreu et al. Techniques for Measuring Aerosol Attenuation using the Central Laser Facility at the Pierre Auger Observatory. *JINST*, 8:P04009, 2013, 1303.5576.

[18] S.Y. BenZvi, R. Cester, M. Chiosso, B.M. Connolly, A. Filipcic, et al. The Lidar System of the Pierre Auger Observatory. *Nucl.Instrum.Meth.*, A574:171–184, 2007, astro-ph/0609063.

[19] J. Chirinos for the Pierre Auger Collaboration. Cloud Monitoring at the Pierre Auger Observatory: Contribution to the International Cosmic Ray Conference (ICRC 2013). 2013, 1307.5059.

[20] Pedro Abreu et al. Identifying Clouds over the Pierre Auger Observatory using Infrared Satellite Data. *Astropart.Phys.*, 50-52:92–101, 2013, 1310.1641.

[21] Georges Aad et al. Search for displaced vertices arising from decays of new heavy particles in 7 TeV pp collisions at ATLAS. *Phys.Lett.*, B707:478–496, 2012, 1109.2242.

[22] B.C. Allanach, M.A. Bernhardt, H.K. Dreiner, C.H. Kom, and P. Richardson. Mass Spectrum in R-Parity Violating mSUGRA and Benchmark Points. *Phys.Rev.*, D75:035002, 2007, hep-ph/0609263.

[23] Savas Dimopoulos, Michael Dine, Stuart Raby, and Scott D. Thomas. Experimental signatures of low-energy gauge mediated supersymmetry breaking. *Phys.Rev.Lett.*, 76:3494–3497, 1996, hep-ph/9601367.

[24] JoAnne L. Hewett, Ben Lillie, Manuel Masip, and Thomas G. Rizzo. Signatures of long-lived gluinos in split supersymmetry. *JHEP*, 0409:070, 2004, hep-ph/0408248.

[25] Matthew J. Strassler and Kathryn M. Zurek. Echoes of a hidden valley at hadron colliders. *Phys.Lett.*, B651:374–379, 2007, hep-ph/0604261.

[26] Boaz Keren-Zur, Luca Mazzucato, and Yaron Oz. Direct Mediation and a Visible Metastable Supersymmetry Breaking Sector. *JHEP*, 0810:099, 2008, 0807.4543.

[27] Philip Schuster, Natalia Toro, and Itay Yavin. Terrestrial and Solar Limits on Long-Lived Particles in a Dark Sector. *Phys.Rev.*, D81:016002, 2010, 0910.1602.

[28] D. Heck, G. Schatz, T. Thouw, J. Knapp, and J.N. Capdevielle. CORSIKA: A Monte Carlo code to simulate extensive air showers. 1998.

[29] P. K. F. Grieder. *Extensive Air Showers: High Energy Phenomena and Astrophysical Aspects - A Tutorial, Reference Manual and Data Book*. Springer, August 2010.

[30] J. Chirinos. Ground-truthing a satellite-based night-time cloud identification technique at the Pierre Auger Observatory. *Eur.Phys.J.Plus*, 127:93, 2012.

[31] D. Nitz J. Chirinos T. Yapici, B. Fick and N. Dhital. Tank simulations to investigate the decrease in A/P. *Auger internal report GAP-2012-152*, 2012.

Recent Refereed Publications

The publications listed below are all "full author list" Auger Collaboration papers, and as such involve support from multiple countries and funding agencies. We have excluded from this list Auger papers in which we had minimal involvement.

- "A search for point sources of EeV photons", Pierre Auger Collaboration, Apj, **789** (2014) 160.
- "A Targeted Search for Point Sources of EeV Neutrons", Pierre Auger Collaboration, ApJ, **789** (2014) L34.
- "Identifying Clouds over the Pierre Auger Observatory using IR Satellite Data", Pierre Auger Collaboration, Astroparticle Physics **50-52** (2013) 92-101.
- "Bounds on the density of sources of ultra-high energy cosmic rays from the Pierre Auger Observatory", Pierre Auger Collaboration, JCAP **05** (2013) 009.
- "Techniques for Measuring Aerosols using the Central Laser Facility at the Pierre Auger Observatory", JINST **8**, (2013) P04009.
- "Ultra-High Energy Neutrinos at the Pierre Auger Observatory", Pierre Auger Collaboration, Advances in High Energy Physics, 2013 (2013) 708680.
- "The Interpretation of the Depths of Shower Maximum of Extensive Air Showers Measured by the Pierre Auger Observatory", Pierre Auger Collaboration, JCAP **02**, (2013) 026.
- "Constraints on the origin of cosmic rays above 10^{18}eV from large scale anisotropy searches in data of the Pierre Auger Observatory", Pierre Auger Collaboration, Ap. J. Lett. **762** (2013) L13.
- "Large scale distribution of arrival directions of cosmic rays detected above 10^{18}eV at the Pierre Auger Observatory", Pierre Auger Collaboration, Ap. J. Suppl. **203** (2012) 34.
- "A Search for Point Sources of EeV Neutrons", Pierre Auger Collaboration, Ap. J. **760** (2012) 148.
- "The Rapid Atmospheric Monitoring system of the Pierre Auger Observatory", Pierre Auger Collaboration, JINST **7** (2012) P10011.
- "Measurement of the proton-air cross-section at $\sqrt{s}$=57 TeV with the Pierre Auger Observatory", Pierre Auger Collaboration, Phys. Rev. Lett. **109** (2012) 062002.
- "Search for point-like sources of ultra-high energy neutrinos at the Pierre Auger Observatory and improved limit on the diffuse flux of tau neutrinos", Pierre Auger Collaboration, Ap. J. Lett. **755** (2012) L4.
- "A search for anisotropy in the arrival directions of ultra high energy cosmic rays recorded at the Pierre Auger Observatory", Pierre Auger Collaboration, JCAP **04** (2012) 040.

- “Description of Atmospheric Conditions at the Pierre Auger Observatory using the Global Data Assimilation System (GDAS)”, Pierre Auger Collaboration, Astroparticle Physics **35** (2012), 591-607.
- “Search for signatures of magnetically-induced alignment in the arrival directions measured by the Pierre Auger Observatory”, Pierre Auger Collaboration, Astroparticle Physics **35** (2012) 354.
- “Search for ultrahigh energy neutrinos in highly inclined events at the Pierre Auger Observatory”, Pierre Auger Collaboration, Phys. Rev. **D84** (2011) 122005.
- “The effect of the geomagnetic field on cosmic ray energy estimates and large scale anisotropy”, Pierre Auger Collaboration, JCAP **11** (2011) 022.
- “The Lateral Trigger Probability function for UHE Cosmic Ray Showers detected by the Pierre Auger Observatory”, Pierre Auger Collaboration, Astroparticle Physics **35** (2011) 266-276.
- “Anisotropy and chemical composition of ultra-high energy cosmic rays using arrival directions measured by the Pierre Auger Observatory”, Pierre Auger Collaboration, JCAP **6**, (2011) 22.
- “Search for First Harmonic Modulation in the Right Ascension Distribution of Cosmic Rays Detected at the Pierre Auger Observatory”, Pierre Auger Collaboration, Astroparticle Physics **34** (2011) 627-639.
- “The exposure of the hybrid detector of the Pierre Auger Observatory”, Pierre Auger Collaboration, Astroparticle Physics **34** (2011) 368-381.